This is the post-print version of the following article: *Nattida Chotechuang, Paolo Di Gianvincenzo, Cheng Giuseppe Chen, Alessandro Nicola Nardi, Daniel Padró, Chanchai Boonla, Maria Grazia Ortore, Marco D' Abramo, Sergio E. Moya, A study of cyanidin/alginate complexation: Influence of pH in assembly and chiral properties*. ***Carbohydrate Polymers**, 2023*

DOI: https://doi.org/10.1016/j.carbpol.2023.120957

This article may be used for non-commercial purposes in accordance with Elsevier Terms and Conditions for Self-Archiving.

© <2023>. This manuscript version is made available under the CC-BY-NC-ND 4.0 license http://creativecommons.org/licenses/by-nc-nd/4.0/

A study of cyanidin/alginate complexation: influence of pH in assembly and chiral properties.

Nattida Chotechuang [a,b], Paolo Di Gianvincenzo [b], Cheng Giuseppe Chen [c], Alessandro Nicola Nardi [c], Daniel Padró [b], Chanchai Boonla [d], Maria Grazia Ortore [e], Marco D' Abramo [c], Sergio E. Moya [b]

[a] Department of Food Technology, Faculty of Science, Chulalongkorn University, 10330, Bangkok, Thailand

[b] Center for Cooperative Research in Biomaterials (CIC biomaGUNE), Basque Research and Technology Alliance (BRTA), Paseo Miramon 182 C, 20014, Donostia-San Sebastian, Spain

[c] Chemistry Department, ''La Sapienza'' University of Rome, P.le A. Moro 5, 00185, Rome, Italy

[d] Department of Biochemistry, Faculty of Medicine, Chulalongkorn University, 10330, Bangkok, Thailand

[e] Department of Life and Environmental Sciences, Marche Polytechnic University, Via Brecce Bianche, I-60130, Ancona, Italy

Corresponding author: Sergio E. Moya, CIC biomaGUNE, Paseo Miramon 182 C, 20014, Donostia-San Sebastian, Spain. E-mail address: smoya@cicbiomagune.es. Telephone: +34 943 00 53 11

Journal Pre-proof

Abstract

Cyanidin 3-O-glucoside (CND) is a frequently-used anthocyanin that has excellent antioxidant properties but a limited bioavailability in bloodstream. Complexation of CND with alginate can improve its therapeutic outcome. Here we have studied the complexation of CND with alginate under a range of pH values from 2.5 to 5. CND is positively charged at low pH, and becomes neutral, and then negatively charged as pH increases. CND/alginate complexation was studied by dynamic light scattering, transmission electron microscopy, small angle X-ray scattering, STEM, UV-Vis spectroscopy and circular dichroism (CD). CND/alginate complexes at pH 4.0 and 5.0 form chiral fibres with a fractal structure. At these

pH values, CD spectra show very intense bands, which are inverted compared with free CND. Complexation at lower pH results in disordered polymer structures and CD spectra show the same features as for CND in solution. Molecular dynamics simulations suggest the formation of parallel CND dimers through complexation with alginate at pH 3.0, while at pH 4.0 CND dimers form in a cross like arrangement.

Keywords

Anthocyanins, alginate, complexation, chirality, fibres, molecular dynamics

1. Introduction

Anthocyanins are secondary metabolites from plants responsible for the orange, red, purple, and blue colours of flowers and fruits, and the red colours of autumn leaves. They are also molecules of large therapeutic interest, widely applied because of their antioxidant, antiaging, anti-inflammatory, antidiabetic, and anticancer properties (Olivas-Aguirre et al., 2016; Rupasinghe et al., 2018). However, a very low bioavailability of anthocyanins is the main challenge for their medical application. Cyanidin 3-O-glucoside (CND) is one of the most abundant anthocyanins, found in edible pigment plants such as berries, purple grapes, purple potatoes, butterfly pea flowers, roselle and others.

The structure and colours of CND strongly depend on the pH. At acidic pH ≤ 3, the red-orange flavylium cation (AH^+) is the only species present; however, as pH increases, the flavylium cation undergoes chemical tautomerism and protonation that lead to distinct molecular structures that are no longer positively charged (neutral quinoid base), and can even become negatively charged (anionic quinoid base) at higher pH values (Fig. 1A) (Pina, 2014; Pina et al., 2012).

Journal Pre-proof

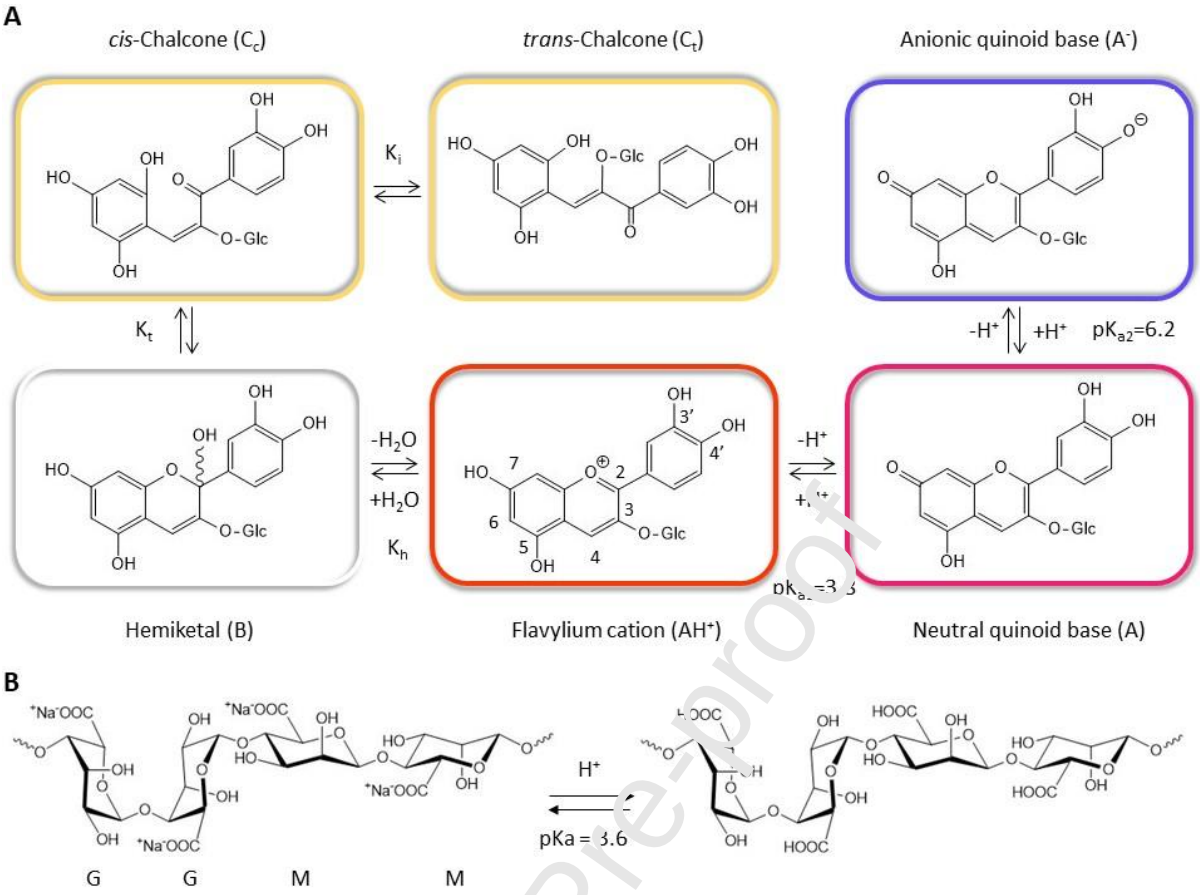

Fig. 1. A) Cyanidin 3-O-glucoside structures according to degree of protonation. At pH higher than 3, the flavylium cation (AH^+) undergoes sequential deprotonations resulting in the neutral quinoid base (A) and blue-purple anionic quinoid base (A^-). On the other hand, nucleophilic addition of water leads to the colourless hemiketal (B), with subsequent tautomerization to *cis*-chalcone and isomerization to *trans*-chalcone with equilibrium constants K_h, K_t and K_i respectively. B) Sodium alginate in equilibrium with alginic acid. M and G represent mannuronic acid and guluronic acid monosaccharide blocks, respectively.

At pH >3 the most abundant isomer of CND is the neutral quinonoid (A) due to the deprotonation of C7-OH, the most acidic group. At higher pH, a second proton loss from C4'-OH results in the anionic quinoid base (A^-). While deprotonations progressively result in the purple-blue quinoidal base, the flavylium cation (AH^+) can also undergo nucleophilic addition of water to the C2 position. This reaction produces the colourless hemiketal (B) and, through tautomerization, the yellow *cis*-chalcone (C_c) that isomerizes to *trans*-chalcone (C_t). Although hydration is thermodynamically more favourable than deprotonation it is also much slower. All these reactions are in equilibrium, and the acidification to pH 2.0-3.0 reverts the system to the cationic form AH^+, recovering the colour (Quina et al., 2009).

Journal Pre-proof

Anthocyanins are also planar compounds capable of associating among themselves by non-covalent interactions through their aromatic rings. Self-aggregation of anthocyanidin depends on pH and concentration (Gavara et al., 2013; Leydet et al., 2012; Trouillas et al., 2016). Dimer formation in solution should take place at concentrations over 1 mM in both flavylium cation and neutral quinonoid bases (Asen et al., 1972; Dangles & Fenger, 2018; Hoshino, Matsumoto, & Goto, 1981; Hoshino, Matsumoto, Harada, et al., 1981; Houbiers et al., 1998). The presence of glucose on C3 and C5 enhance self-association due to additional hydrogen bonds (Houghton et al., 2021). However, weaker association is observed by the hemiketal and chalcone forms due to decreased conjugation of the tricyclic core upon ring opening.

Since cyanidin has an isomeric form with a positive charge, the flavylium ion, we decided to perform the encapsulation with alginate, a negatively charged polysaccharide, by electrostatic complexation (Fig. 1B). Alginate is the salt of alginic acid, found in algae. It is highly hydrophilic and biocompatible, and widely used in food formulations. Previous reports show that alginate is a good candidate for CND complexation (Zou et al., 2021); it is a linear copolymer with homopolymeric blocks of (1→4)-linked β-D-mannuronate (M) and α-L-guluronate (G) residues covalently linked together in different sequences, which can include homopolymeric blocks of consecutive G residues, consecutive M-residues (M-blocks), or alternating M and G residues (Fig. 1B). Alginate has one carboxylate group per monosaccharide; it is a weak polyanion and its charge depends on pH (pKa = 3.6). It is highly negatively charged at basic pH but loses charges at acidic pH, where CND becomes positive.

CND has the drawback of being an unstable compound and rapidly degrades when exposed to neutral and basic pH values, high temperature, and in the presence of oxygen (Francis & Markakis, 1989). CNDs are usually administrated orally. While stable at acid pH, such as in the stomach, CNDs are prone to enzymatic degradation. Following stomach digestion, CND will encounter the basic environment of the small intestine, which further acts on CND degradation. Consequently, bioavailability of CND in blood is low, limiting therapeutic outcome (Oidtmann et al., 2012; Yi et al., 2006). Co-pigmentation is a naturally occurring stabilization mechanism based on non-covalent interactions of anthocyanins with colourless organic molecules (Asen et al., 1972). A polymeric matrix to encapsulate CND would help to protect the CNDs by acting as a co-pigment. Since anthocyanins are bio-synthesized in a polysaccharide rich environment (Fernandes et al., 2016), the entrapment of CND within polysaccharide chains seems to be a logical approach. Moreover, polysaccharides are frequently used as micro/nanostructured additives for food, benefiting from their chemical

versatility, biocompatibility and abundance. Our first attempt was to form CND/alginate complexes by varying pH in a range where both CND and alginate are charged. Complexes were successfully prepared at pHs from 2.5 to 5.0, and their physicochemical properties noticeably depended on pH. Most interestingly, the chirality of CND/alginate complexes differed significantly over the range of pH values tested. Circular dichroism (CD) spectra of the complexes showed much more intense bands than the free CND. Some bands in the spectra of the complexes are absent in the spectra of CND in solution, suggesting a supramolecular organization of CND driven by its interaction with alginate. The motivation of this work is to better understand the interaction of CND with alginate and how pH affects this interaction, which is fundamental for the design of polysaccharide-based CND carriers. Our working hypothesis is that the changes in the structure of CND with pH will lead to a different association between CNDs and alginate and among CND molecules complexed with alginate, resulting in structures with different molecular organization and chiral properties at the different pHs considered. CND/alginate complexes were characterized by ultraviolet-visible spectroscopy (UV-Vis), dynamic light scattering (DLS), scanning transmission electron microscopy (STEM), CD, and small angle X-ray scattering (SAXS). Molecular dynamic simulations were used to study the interaction of CND with alginate, providing fundamental insight into the interaction behaviour of charged and non-charged CND in the presence of alginate.

2. Materials and methods

2.1. Reagents

Cyanidin 3-O-glucoside (MW = 484.84 g/mol) and alginate sodium salt low viscosity (A1112, Mw = 51 KDa and Mn = 27 KDa, G/M:3) (Jeoh et al., 2021), were purchased from Sigma-Aldrich with purity >99% and used without further purification. Carbon-coated copper grids and uranyl acetate were purchased from Electron Microscopy Sciences (USA). Water used for all the experiments was ultrapure MilliQ water.

2.2. Dynamic light scattering (DLS)

DLS measurements were performed with a Zeta Sizer Ultra Malvern Instrument in backscattering mode. All studies were performed at a controlled temperature of 25 °C using disposable folded capillary cells (DST1070). Alginate and CND/alginate complexes were

characterized for size and ζ-potential. Each sample was measured in triplicate at a concentration of 0.25 mg/mL in MilliQ water at pH 2.5, 3.0, 3.6, 4.0 and 5.0.

2.3. Scanning transmission electron microscopy (STEM)

Transmission electron microscopy analysis was performed with a JEOL JEM-2100F UHR microscope operating at an acceleration voltage of 200 kV. Carbon films (Aname, CF400-CU) were pre-treated in a glow discharged chamber Emitek K100X (2 minutes, 35 mA). All samples (alginate and CND/alginate) were deposited on plasma treated carbon grids (0.01 mg/mL, 0.5 µL) for 1 minute. Staining was carried out with uranyl acetate (0.5%, 0.5 µL) with 1 minute incubation and subsequent washing with 5 µL of MilliQ water at corresponding pH.

2.4. Ultraviolet-visible spectroscopy (UV-Vis) and circular dichroism (CD)

UV-Vis spectra were recorded using a JASCO V-730. The full spectrum (190–700 nm) for each sample was recorded at room temperature. Alginate (1 mg/mL) and CND/alginate (0.4 and 1 mg/mL) were dissolved in N_2 purged MilliQ water at pH 2.5, 3.0, 3.6, 4.0 and 5.0. CD measurements were performed using a JASCO J-1500 CD spectrometer. A quartz cuvette with 1 mm optical pathlength was used for these measurements recording from 190 to 700 nm with a bandwidth of 1 nm at room temperature. Alginate and CND/alginate were dissolved at 1 mg/mL in N_2 purged MilliQ water at pH 2.5, 3.0, 3.6, 4.0 and 5.0. Each CD spectrum was recorded and accumulated three times.

2.5. Small angle X-ray spectroscopy (SAXS)

SAXS experiments were performed at the Austrian beamline at the Elettra Synchrotron, Trieste, Italy. Measurements were carried out at 20 °C in capillaries of 1.5 mm outer diameter/0.01 mm wall thickness made from borosilicate (Hilgenberg, Maisfeld, Germany). The capillary is enclosed within a thermostatic compartment connected to an external circulation bath, and a thermal probe for temperature control. Data for the transmission of the sample and the fluctuations of the primary beam were corrected, the scattering patterns of all the images of each sample were averaged and the respective backgrounds, treated in the same way, were subtracted. A Pilatus3 1M detector system recorded the two-dimensional patterns, processed by SAXSDOG (Burian et al., 2022) and by Igor Pro software (WaveMetrics, Lake Oswego, OR, USA) to obtain radial averages. Bidimensional spectra report the scattering intensity as a function of the magnitude of the scattering vector Q defined as $Q = 4\pi \sin\theta / \lambda$,

with 2θ being the scattering angle and λ equal to 0.154 nm the wavelength of X-rays corresponding to an energy of 8 keV). Alginate and CND/Alginate complexes were measured at a concentration of 1.00 mg/mL in MilliQ water at pH 3.0, 4.0, and 5.0. Each sample was measured at least 18 times with an acquisition time of 10 s and a dwell time of 3 s for each measurement. An average of each set of acquisitions, was obtained after checking for possible radiation damage. No radiation damage was observed for the investigated samples. Both the samples and their buffers were measured under the same conditions regarding temperature and exposure time. To generate model-free results, we firstly plotted SAXS data in the form of Kratky plots. If a well-defined bell-shape can be evidenced in the Kratky plot, it follows that macromolecules in solution show a somehow compact structure. On the other side, if Kratky plot does not show a clear peak, just disordered species are observed. Since we observed both cases, two data analysis approaches were adopted to fit SAXS experimental curves. Data corresponding to disordered species in solution (evidenced by the lack of a peak in Kratky plot) were analysed by the form factor of a randomly oriented Gaussian-chain, which is expressed by Debye's law, whose unique free parameter is the gyration radius *Rg*. Data corresponding to well-formed species, as demonstrated by the presence of a peak in Kratky plot, were analyzed by Beaucage model of polymeric mass fractals (Beaucage 1996). This model accounts for the large-scale polymer coil size (R_g), composed of small-scale Kuhn steps of size R_S. Hence, two structural levels were considered: a large scale structural level corresponding to the chain, which is composed of a small scale structural level, the rod subunits corresponding to Kuhn segments whose size, R_S, is a fitting parameter. Both the models are applied to the full experimental q-range (Polizzi et al., 2015), and SAXS data were analyzed by GENFIT software (Spinozzi et al., 2014).

2.6. Molecular dynamics (MD) simulations

NVT MD simulations of two AH^+ or two A molecules in aqueous solution in the presence of different models of alginate were performed at a temperature of 300 K, using the force field CGenFF/CHARMM36 (Vanommeslaeghe et al., 2010) and TIP3P as the water model. The force field parameters for AH^+ and A were obtained through CHARMM-GUI (Jo et al., 2008), using the ESP charges (Singh & Kollman, 1984) obtained by DFT calculations at the ωB97XD/6-311+G* level (Chai & Head-Gordon, 2008), using geometries minimized at the ωB97XD/6-31G(d) level. In the cases where such an automatic process failed to generate suitable parameters, they were estimated using the ones found in CGenFF (Jo et al., 2008), based on chemical similarity. The polymers used as models of alginate were pure guluronic

(G_{20}), pure mannuronic (M_{20}), block copolymers of guluronic and mannuronic ($G_{10}M_{10}$)and random guluronic mannuronic alginates $(GM)_{10}$, considered in their deprotonated form. The systems were neutralized by adding the necessary amount of Na^+ ions. Rhombic dodecahedron boxes of around 70 nm^3 of volume containing around 21,000 molecules of solvent were considered (the volumes used reproduce the experimental condition of the isobaric insertion of the solute in liquid water at infinite dilution) (Del Galdo et al., 2015). The canonical sampling was obtained using the velocity rescaling thermostat (Bussi et al., 2007). Periodic boundary conditions were adopted, setting a cut-off of 1.1 nm for the short-range interactions, while the long-range interactions were calculated using the Particle Mesh Ewald method (Darden et al., 1993) using a cut-off of 1.1 nm. For each system, 3 simulations of 200 ns from randomly obtained initial conditions were performed with a timestep of 2 fs. The MD simulations were carried out using Gromacs 2021.5 (Abraham et al., 2015), while the DFT calculations were performed using Gaussian16 (Frisch et al., 2016). CNDs were considered dimers when the minimum distance between two atoms of each molecule is less than 0.4 nm.

The same criteria and cut-off value (i.e. 0.4 nm) have been applied to determine whether the CNDs are bound to alginate. For the conformational analysis of the CND dimer bound to alginate, we evaluated the MD sampled distributions of i) the scalar product of the versors corresponding to the vectors $\vec{v}_1$ and $\vec{v}_2$, indicating the mutual orientation between the two cyanidin molecules (see Fig. 7D), ii) the sum of the distances $\vec{d}_1$ and $\vec{d}_2$, indicating the degree of planar shift between the two monomers (see Fig. 7C), and iii) the scalar product of the versors corresponding to the vectors obtained by the cross product of $\vec{v}_1$ and $\vec{u}_1$, and of $\vec{v}_2$ and $\vec{u}_2$ (where $\vec{u}_1$ and $\vec{u}_2$ are the vectors that connect the carbon atoms in position 2 and 3, see Fig. 1A; together with $\vec{v}_1$ and $\vec{v}_2$, they identify the planes approximating the benzopiranoil moieties of CND), indicating if the monomers are stacked facing each other on the same side or not, i.e. if the cyanidins are placed as a specular pair or not, see Fig. 7B; we will simply refer to it as "Cross product":$(\vec{v}_1 \times \vec{u}_1)$. ($\vec{v}_2 \times \vec{u}_2$) .
We later applied a Kernel density estimation to the sampled distributions (see Fig. 7A). The most significant conformation for A and AH^+ (see Fig. 7B and Fig. 7C) have been obtained by performing a k-means clustering (Lloyd, 1982) using the standardized sampled values of scalar product, sum of distances and cross product along the simulations, using 4 clusters for A and 2 clusters for AH^+ (see Fig. S3B in SI), as determined by applying the “elbow” rule by plotting the inertia against the number of clusters used in the analysis (see Fig. S3A in SI).

3. Results and discussion

3.1. CND/alginate complex preparation

Fig. 1 shows the chemical structures of CND and alginate, and the different tautomeric forms of CND according to pH. CND/alginate complexes were prepared varying pH from 2.5 to 5.0 to find the optimum conditions for association between CND and alginate. Complexes were prepared using a procedure based on Zou's protocol (Zou et al., 2021) with some modifications. The pH range was chosen taking into account the pK_as of alginate (~3.5) and CND (~3.8), and the pH range where both molecules, or at least one of them, is charged. MilliQ water was adjusted to pH 2.5, 3.0, 3.6, 4.0, and 5.0 with HCl 0.1 M and purged 30 minutes with N_2 just prior to use. PH was adjusted with HCl as it was preferred not to use buffers to avoid any potential effect of the salts of the buffer in the complexation process. Alginate and cyanidin were dissolved in MilliQ water at the selected pHs to a concentration of 1 mg/mL. Then, pH was monitored and eventually adjusted to the desired value. To determine the maximum amount of CND that can be complexed with alginate, four CND/alginate complexes with different CND/alginate monomer ratios were prepared (1:10, 1:50 and 1:100). As monomer ratios we mean the ratio between mmol of CND to mmol of alginate monomers. We finally used 1:10 ratio because in this condition we found a small amount of precipitate indicating the saturation of alginate with CND. CND and alginate solutions were precooled in ice, and then mixed under inert atmosphere with a ratio of CND to alginate monomers equal to 1:10. In a typical complexation reaction, CND solution (82.5 µL; 1 mg/mL; $1.7 \cdot 10^{-4}$ mmol) was added dropwise to the alginate solution (300 µL; 1 mg/mL; $1.7 \cdot 10^{-3}$ mmol of monomer). Mixtures were left under shaking for one hour at 4 °C in the dark. Samples were centrifuged at 10000 rpm for 5 minutes in a Minispin centrifuge. The supernatant solution was separated from precipitates and freeze dried. After weighting the purple solids obtained the amount of soluble CND/alginate complexes could be estimated, which changes depending on pH ranging from 75% at pH 2.5 to 91% at pH 5.0.

3.2. Dynamic light scattering (DLS)

CND/alginate complexes were characterized by DLS. All samples were prepared at 0.25 mg/mL in the corresponding MilliQ water at pH 2.5, 3.0, 3.6, 4.0 and 5.0. The hydrodynamic diameter of alginate alone did not show notable differences when changing the pH (Fig. 2), with a hydrodynamic diameter of 207 nm at pH 2.5, 160 nm at 3.0, and around 300 nm for pH 3.6, 4.0 and 5.0. Size differences are probably due to the internal repulsion of the

increased number of negative charges as pH increases that leads to a less coiled arrangement of the alginate. Alginate's pKa is around 3.6. For the CND/alginate complex, the hydrodynamic diameter determined is almost the same as that of alginate alone at pH 2.5, 3.0, and 3.6. However, there is an abrupt change in CND/alginate size when pH increases to 4.0 and 5.0. The hydrodynamic diameter dramatically increases reaching values of around 1040 nm at pH 4.0 and 1600 nm at pH 5.0 (Fig. 2).

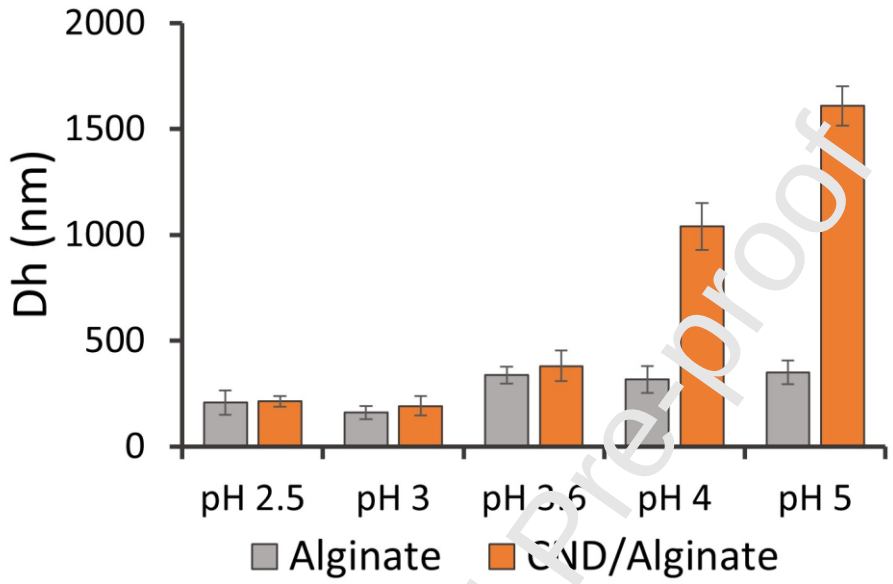

Fig. 2. Hydrodynamic diameters of alginate (grey bars) and CND/alginate complexes (orange bars) obtained by DLS. Both samples correspond to an alginate concentration of 0.25 mg/mL in MilliQ water at pH 2.5, 3.0, 3.6, 4.0 and 5.0. Measurements were performed at 25 °C.

ζ-potential of alginate and CND/alginate complexes at different pHs were measured. As expected, alginate gave negative ζ-potential values, ranging from -10 (pH 2.5) to -50 (pH 5.0). CND/alginate complexes show slightly less negative values compared to the corresponding sample of alginate alone at the same pH.

3.3. Scanning transmission electron microscopy (STEM)

To gain more insight into the structure of the CND/alginate complexes as we varied pH, STEM experiments were performed. STEM images of CND/alginate complexes at pH 4.0 and 5.0 showed sizes in agreement with data obtained by DLS (Fig. 3A and 3C). Even though morphology is slightly different at the two pH values tested, in both cases we observe the formation of thin fibres that seem to follow a fractal geometry.

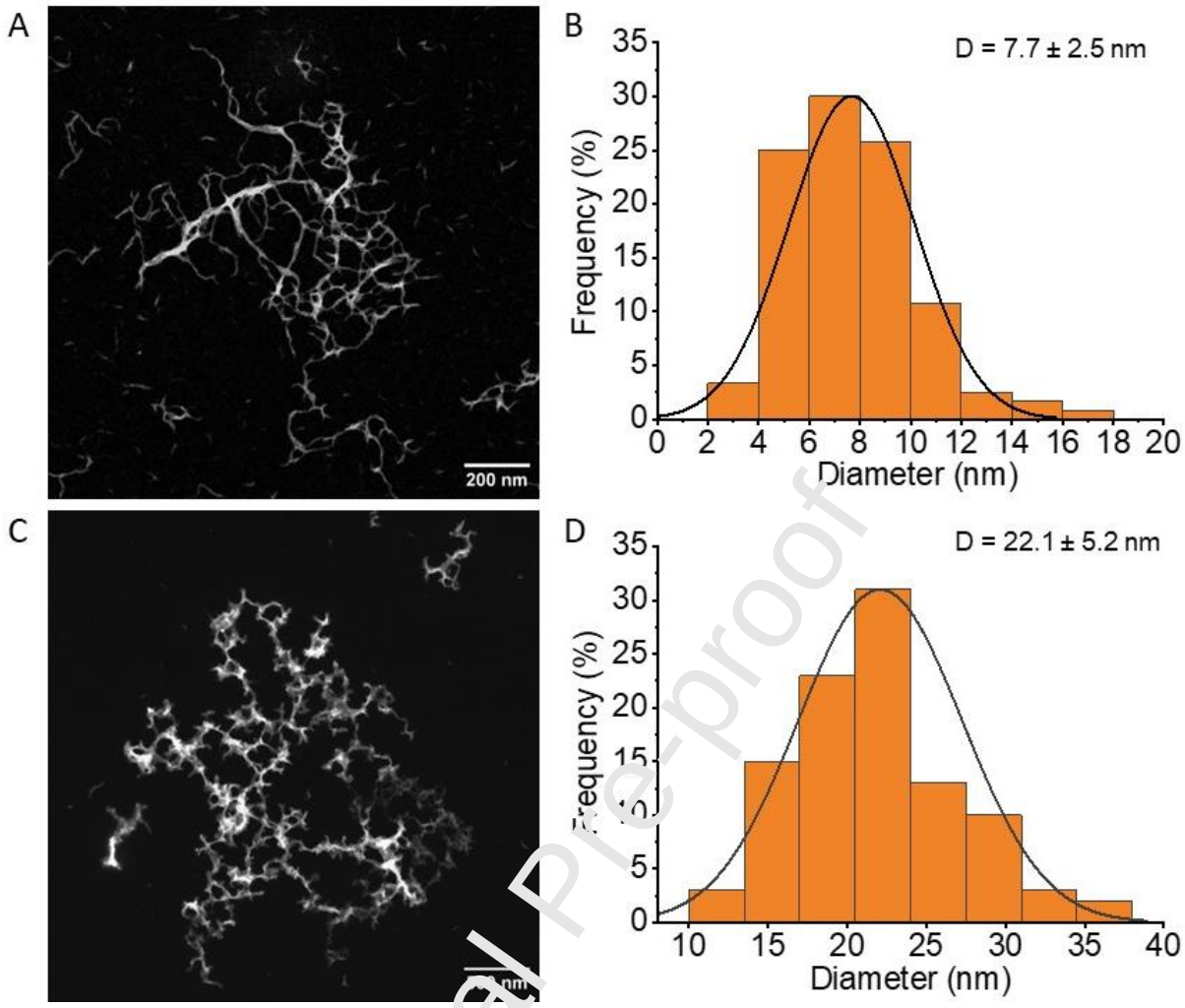

Fig. 3. STEM characterization of CND/alginate. Samples were prepared on activated carbon grids and stained with a 0.5% solution of uranyl acetate. A) CND/alginate at pH 4.0 (scale bar: 200 nm). B) Histogram representing fibre diameter of CND/alginate at pH 4.0 nanostructure (100 fibre diameters were measured, with an average diameter of 7.7 ± 2.5 nm). C) CND/alginate at pH 5.0 (scale bar: 500 nm). D) Histogram representing fibre diameter of CND/alginate at pH 5.0 nanostructure (120 fibre diameters were measured with an average diameter of 22.1 ± 5.2 nm)

Fibre diameters of CND/alginate at pH 4.0 and pH 5.0 were measured. CND/alginate complexes at pH 5.0 show an average fibre diameter of 22.1 ± 5.2 nm (Fig. 3D); almost three times larger than the fibres seen at pH 4.0, which have an average diameter of 7.7 ± 2.5 nm (Fig. 3B). CND/alginate complexes at pH 2.5 and 3 did not show any organized structure, and just a few straight fibres were found in the case of CND/alginate pH 3.6 (Fig. S1). As a control, STEM experiments were also carried out with alginate alone in MilliQ water at pH 2.5, 3.0, 3.6, 4.0 and 5.0. No structure resembling the CND/alginate complexes was found for alginate alone.

3.4. Small angle X-ray scattering (SAXS)

Synchrotron SAXS experiments were performed on alginate and CND/alginate complexes at pH 3.0, 4.0, and 5.0. At pH 3.0, SAXS curves corresponding to free alginate and to CND/alginate almost overlap, whereas at pH 4.0 and 5.0 the SAXS fingerprints of CND/alginate dramatically change from those of free alginate, in agreement with DLS results. SAXS curves corresponding to alginate in solution were successfully fitted by adopting the Gaussian-chain model, which resembles a disordered polymer, obtaining a gyration radius for alginate of 2.4 ± 0.1 nm at pH 4.0 and 2.3 ± 0.1 nm at pH 5.0 (purple points in Fig. 4). The complexation of CND and alginate can be clearly seen in Fig. 4 since the features of the SAXS curves are very different. CND/alginate complexes show a SAXS fingerprint typical of fractal structures, and they were consequently analysed by the Beaucage model (Beaucage, 1996). CND/alginate complexes at pH 4.0 show a radius of gyration of 52 ± 1 nm, corresponding to the large-scale polymer coil size, while at pH 5.0 the radius increases to 69 ± 2 nm. The small-scale Kuhn steps of size R_S obtained by Beaucage analysis were of a few nanometres, affected by a considerable error bar. SAXS data analysis confirms the fractal structure for CND/alginate complexes suggested by STEM characterization.

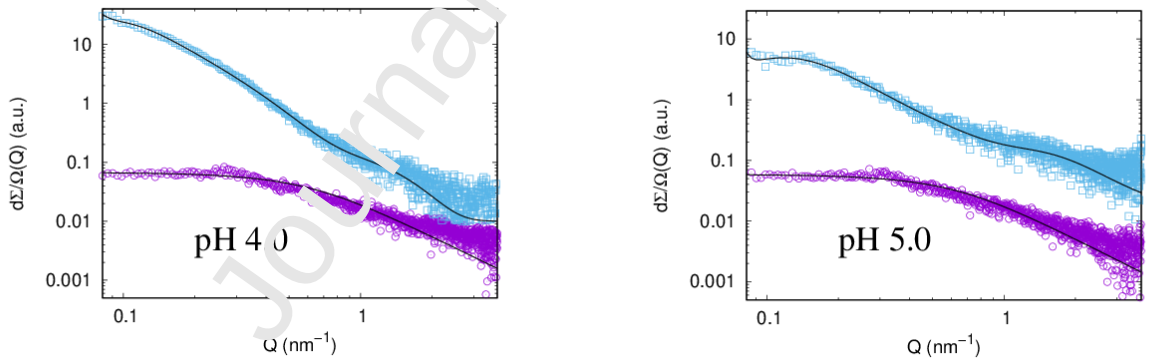

Fig. 4. SAXS curves corresponding to alginate and to CND/alginate at 1 mg/mL at A) pH 4.0 and B) 5.0. Purple circles refer to alginate, cyan squares to CND/alginate; curves are scaled for clarity. Black continuous lines indicate the theoretical fit corresponding to a Gaussian-chain model for alginate samples, and to fractal structures for CND/alginate complexes.

3.5. UV-Vis spectroscopy and circular dichroism (CD)

UV-Vis spectroscopy was carried out on CND, alginate and CND/alginate complexes in a wavelength range from 190-700 nm (Fig. 5 and Fig. S2). Each sample was dissolved in N_2 purged MilliQ water at pH 2.5, 3.0, 3.6, 4.0 and 5.0. UV-Vis spectra of CND (1 mg/mL) and

alginate (1 mg/mL) are in agreement with data found in the literature (Fig. S2). UV-Vis spectra of alginate do not change in response to varying the pH, showing only a weak band around 220 nm. UV-Vis spectra of CND (Fig. 5A) change with pH. Intensity of bands at 280 nm and 508 nm gradually decrease from pH 2.5 to pH 5.0. Moreover, at pH 5.0, the band at 508 nm shifts to 530 nm. A new band at 230 nm appears in the spectra at pH 4.0 and pH 5.0 suggesting disappearance of the flavylium cation AH^+ in favour of C_c and C_t chalcone CND forms. UV-Vis spectra of the CND/alginate complex showed bands of CND and alginate (Fig. 5B). The bands at 508 and 435 nm are present in free CND. However, unlike free CND, these bands at 508 and 435 nm for CND/alginate, do not decrease at the higher pH values of 3.6, 4.0 and 5.0. On the contrary, they almost show a constant intensity. At higher pH, the band at 280 nm also has different behaviour for the complex compared to free CND. CND/alginate at pH 4.0 and 5.0 shows the highest intensity suggesting an increased hydrolysis of benzopiranoil and implying that CND in the complex is present in the *cis* or *trans*-chalcone forms (Fig. 1) that absorb in the same catechol UV region. However, the increase in intensity of the bands at 280 could also result from the scattering of the samples, which is more intense at pH 4 and 5 than at pH 3 as we have seen from SAXS measurements. Nevertheless, an increase of the bands at 280 due to scattering would imply that the intensity of the whole spectra will increase but this is not the case since the band at 508 shows the lowest intensity at pH 4 and 5 among the 4 pHs considered. The differences in UV spectra at these pHs can be clearly visualised in the different coloration of the CND free in solution (Fig. 5A) or complexed with alginate (Fig. 5B). CND alone shows a more intense red colour at low pH, which disappears completely at pH 5.0. CND/alginate complexes have less intense coloration, are red only at pH 2.5 and at higher pH practically do not change colour remaining slightly orange until pH 5.0, a behaviour not observed for CND alone.

Journal Pre-proof

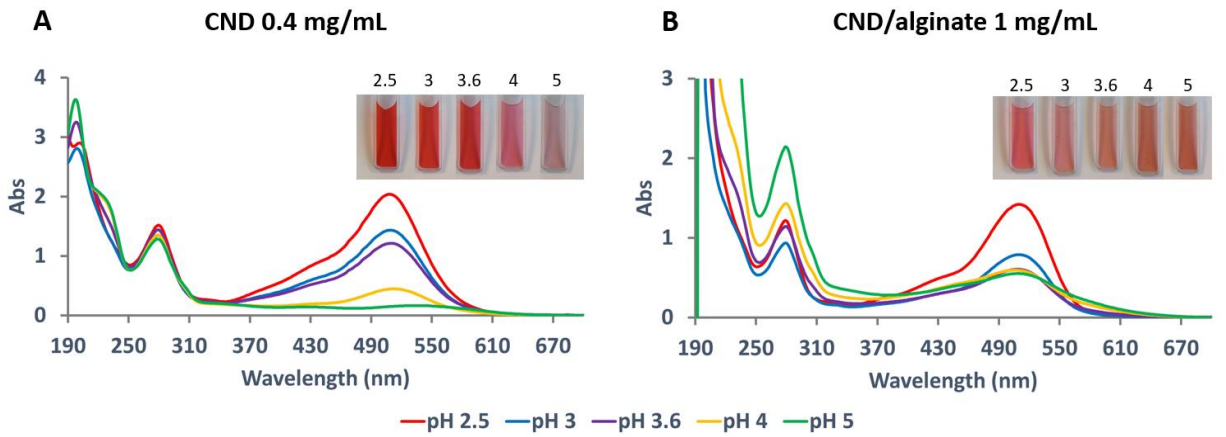

Fig. 5. UV-vis spectra of A) CND 0.4 mg/mL and B) CND/alginate complex (1 mg/mL) both dissolved in N_2 purged MilliQ water at pH 2.5 (red), 3.0 (blue), 3.6 (purple), 4.0 (yellow) and 5.0 (green). Insets show pictures of the CND (A) and CND/alginate (B) solutions at different pH where the changes in colour of CND can be appreciated.

CD spectra of alginate, CND and CND/alginate complexes at pH 2.5, 3.0, 3.6, 4.0 and 5.0 were recorded. CD spectra of alginate alone showed only one negative band at 214 nm with small changes in intensity of this band observed at the different pHs studied (Fig. S2B). Spectra of CND alone are characterized by three negative bands at 215, 280 and 550 nm and two positive bands around 440 and 485 nm (Fig. 6A). Intensity of signals in the 315-620 nm

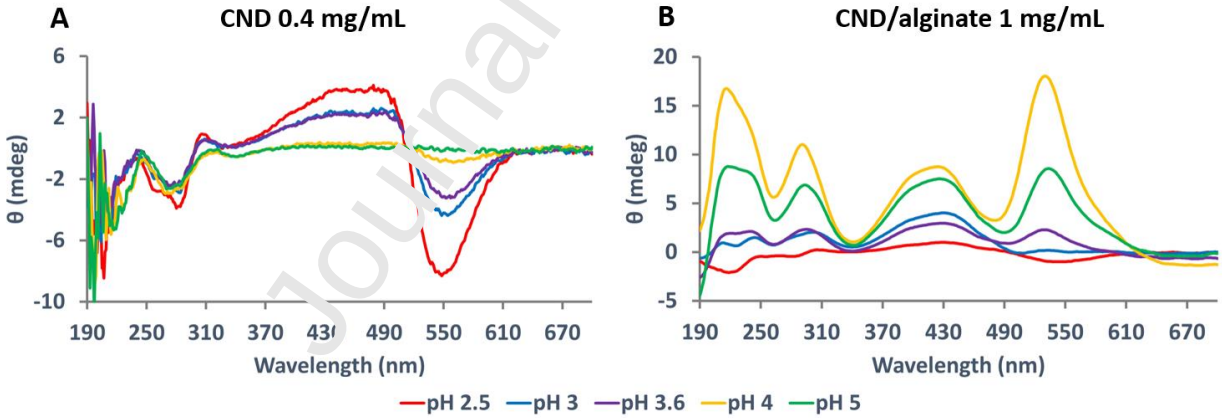

region gradually decrease with increasing pH, and at pH 5.0 almost no signals were observed.

Fig. 6. CD spectra of A) CND 0.4 mg/mL and B) CND/alginate complex (1 mg/mL) both dissolved in N_2 purged MilliQ water at pH 2.5 (red), 3.0 (blue), 3.6 (purple), 4.0 (yellow) and 5.0 (green).

As described in the literature, the colour and chiroptical properties of 3-O-glucoside anthocyanins strongly depend on concentration and pH. Our data for free CND at 0.4 mg/mL and 1 mg/mL at pH values from 2.5 to 5.0 (Fig. 6A and Fig. S2A) are in line with those reported in the literature, indeed, CD signal is proportional to the concentration of

anthocyanin dimers (Houbiers et al., 1998). The two series of CD spectra are very similar giving the same bands without any shifts. The decrease and eventual absence of bands in the region 360-600 nm are indicative of CND being dominantly in the hemiketal form. In this form the benzopiranoil ring of CND is partially hydrolysed, resonance is reduced (which prevents dimerization), and therefore the characteristic bands observed at lowest pHs tend to disappear. CD spectra of CND at 1 mg/mL has higher intensity showing the presence of dimers also at pH 4.0 and 5.0, while at 0.4 mg/mL no dimers seem to be present at these pHs since no CD signal was observed. These results suggest that in this case, the lower the pH, the higher the CD intensity, meaning that the concentration of dimers is higher.

Binding of CND to alginate dramatically changes its CD spectra (Fig. 6B). In the region of 340-490 nm, spectra of CND/alginate show highest intensity at pH 4.0, and the lowest at pH 2.5. Almost the same occurs at pH 3.6, 4.0 and 5.0 for the band at 530 nm, but for pH 3.0 this band almost disappears. On the contrary, at pH 2.5, the CD spectrum is very similar to that of free CND with a negative band at 530 nm. At pHs 3.6, 4.0 and 5.0 the band of CND/alginate at 530 nm becomes positive, suggesting either a change in the symmetry of the dimers or an arrangement of CND in a chiral structure imposed by the interaction with the alginate. A hint in this direction comes from the very strong bands displayed by CND in the complex at pH 4.0, which are much more intense than at other pHs. At low pH 2.5, the aromatic rings of CND in the flavylium ion can induce dimerization of the CND in bulk through pi stacking, but dimers must place positive charges in opposite positions to minimize repulsion. Association of CNDs over dimers is unlikely because of strong charge repulsion that would result from the several charges involved. Compared with CND alone, the complexation of CND with alginate at pH 3.0-5.0, results in a reversal of the band at 500-590 nm which becomes positive and very strong while the band at 350-490 nm remains similar. The bands are significantly stronger than at pH 2.5 and could be indicating the formation of dimers or species of higher order through the complexation with alginate, which is in agreement with the long fibrillar structures observed by TEM. Since alginate is in its anionic form, it will act as a weak base and favour deprotonation of CNDs. Taking into account the UV data and the colour of the complexes, CND must be present in the neutral quinoid base form in the complexes. In this form of CND, the aromatic benzopiranoil ring and the absence of a charge on the ring as in the flavylium ion could favour association among several CND molecules, which could be the reason for the strong intensity of the bands of the CD spectra. It is also possible that there is association between the hemiketal present in the complexes as observed

in UV and the neutral quinoid. The charge of the flavylium ion, present at lower pHs, imposes the dimers to associate with the charges one opposite the other to minimize electrostatic repulsion. Without that restriction, the CND molecules will dimerize to maximize interactions among them, and mainly the two central rings and eventually the third ring may be involved. The absence of a charge in neutral quinoid form would mean the association of CNDs with alginate takes place through weak interactions, i.e. between the glucose in CND and the sugar rings of alginate, as confirmed by the H-bonds analysis of the MD simulations (see Fig. S5). At pH 5.0, the CD spectra from CND and from the complex display the same pattern as in pH 4.0 but bands are much weaker. The UV spectra and the colour of the complexes hint that CND is present in the same form as at pH 4.0. At pH 5.0 the further deprotonation of the CND would result in a negatively charged species, the anionic quinonoid base. However, this form of CND has a characteristic blue, which is not observed in the complexes. The negative charge is likely to prevent the interaction of CND with the negatively charged alginate and for the complexes only the neutral quinonoid is retained with the alginate. Since this form is less frequent at this pH, the loading of the alginate with CND is lower and the bands of the CD spectra are weaker. It may also be that the CND protonates through the interaction with the alginate, and this would explain the differences in colour with the free CND. It is interesting to note that in TEM images, CND/alginate at pH 5.0 seems to be thicker, but according to SAXS data, with a different fractal size, which could mean a different organization of CND with alginate.

3.6. Molecular dynamics (MD) simulations

To gain additional information on the arrangement of cyanidin molecules on the alginate, MD simulations were performed considering the binding of two cyanidin molecules to an alginate molecule. From the MD simulations different geometrical parameters were calculated as shown in Fig. 7A. These values refer only to the frames of the simulations in which both of the following conditions were met: 1) cyanidins are present as dimers and 2) dimers were found to be bound to the alginate (see section 2.6). Four models of alginate were considered, namely G_{20} (20 units guluronic acid), M_{20} (20 units mannuronic acid), $G_{10}M_{10}$ (block of 10 units guluronic acid and block of 10 units mannuronic acid), and $(GM)_{10}$ (10 random units of mannuronic and guluronic acid).

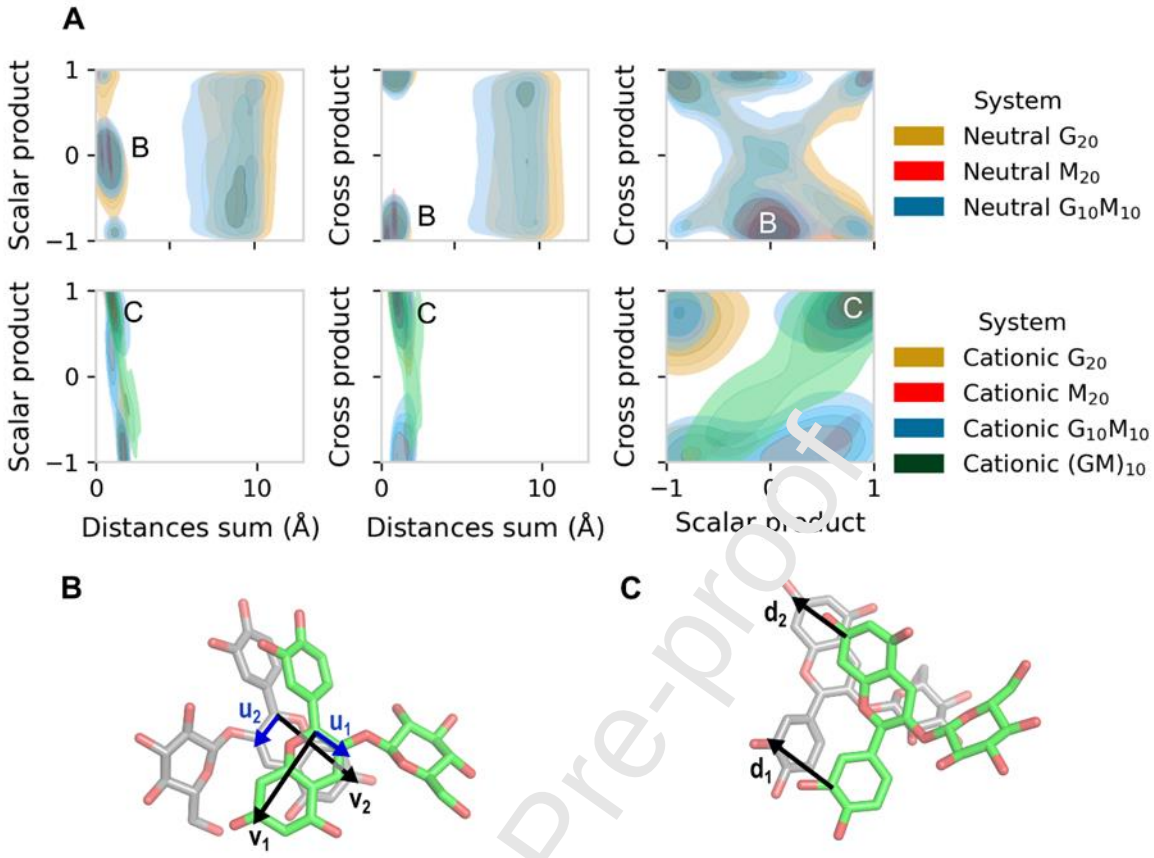

Fig. 7. A) Sampled distributions of the paired values of the "scalar product", "distances sum" and "cross product" (as defined in section 2.6) for each of the systems considered. The most significant conformations obtained by k-means clustering (see section 2.6), and the vectors used in the geometric analysis for B) neutral CND, and C) cationic CND.

We considered alginate molecules purely consisting of guluronic acid and purely composed of mannuronic as the interaction of the cyanidin with one or another block may be different with the G or M residues. Cyanidin was considered in its neutral and cationic state. For each system, three simulations were carried out from different randomly obtained conformational starting points. It is worth noting that the dimerization of the neutral cyanidin was observed for all models except $(GM)_{10}$. To provide a quantitative picture of the interaction behaviour between the cyanidin molecules and the alginate, three parameters were calculated from the MD trajectories, the "scalar product", "distances sum" and the "cross product", as defined in section 2.6.

From MD data it appears that the different cyanidin charge states result in different sets of values of these parameters, indicating that different conformations of the cyanidin dimers - interacting with alginate - are sampled. In particular, neutral cyanidin dimers display a higher

conformational freedom in the subspace defined by the three geometrical parameters, favouring a conformation in which the two monomers can be considered in a cross-like geometry as shown in Fig. 7B. In such a conformation the ortho phenol rings of each cyanidin lie one parallel to the other while the glucose rings point in opposite directions. The fused aromatic rings of the cyanidins are only partially overlapping in this arrangement. Other possible conformations are shown in the supporting information (Fig.S4). For the cationic state, fewer conformations are sampled along the MD trajectories. A shifted parallel dimer was the most sampled in the models considered (see Fig. 7C) and, to a lesser extent, an antiparallel conformation. The structures shown in Fig. 7B and 7C were obtained by performing a k-means clustering. In the shifted parallel conformation, the charge of the fused aromatic rings of cyanidin points in the same direction for the two CND in the dimer, with a high overlap of their aromatic rings, i.e. orto phenolic ring to orto phenolic ring and fused aromatic rings to fused aromatic rings, while the glucose rings lie in a perpendicular plane. The neutral CND dimer in interaction with alginate preferentially found in cross-like conformations (high population around 0 of the scalar product), may correspond to a maximum of the CD signal (which can be assumed to have a dependence on the sinus of the angle between the transition moments ($\vec{\mu}_1$ and $\vec{\mu}_2$) of the two CNDs, according to the: $R \propto -\vec{r} \cdot (\vec{\mu}_1 \times \vec{\mu}_2)$, as described by Cantor and Schimmel (Cantor & Schimmel, 1980), where R is the rotational strength, $\vec{r}$ is the distance between the centres of mass of the two CNDs, and × that indicates the cross product. This is indeed observed in CD spectra. At pH 4.0, CND is present in a non charged form and the CD bands are the strongest. On the other hand, at lower pH, high populations of conformers CND dimers are present as parallel dimers are found with CND in cationic form. In this condition the angle between CND molecules is near 0°, resulting in a low CD signal, as observed experimentally.

The complexation of CND with alginate has shown a rich and unexpected behaviour. In our initial thoughts complexation at lowest pHs of alginate with CND bearing a positive charge should be the most attractive condition for encapsulation since at pH 4.0 and 5.0 the limited charges of CND should not favour association with alginate. However, at these pHs CND/alginate complexes show the most interesting features. Electrostatic complexation interplays with self-association for the formation of the complexes. At pH 4.0 and 5.0, the formation of fibrillar structures with a fractal geometry in the CND/alginate complexes hints at a supramolecular association among the CND, which is not present for free CND in bulk, and which must be induced by the interaction with alginate. It seems that for the charged

flavylium ions at low pH, the strong electrostatic interaction prevents large association of CND in the complexes since these retain the conformational characteristics of free alginate. UV spectra show that the complexation with alginate favours other forms of CND different from the predominant form in solution at the considered pHs, implying a lower local pH in the alginate. Most notably is the increase in the intensity of the hemiketal forms, while with the visual colour of the samples indicates the presence of the neutral quinone base, even at pH 5.0 where it is not predominant. The stabilization of supramolecular CND structures by alginate also leads to interesting chiral properties that should come from the organization of the cyanidin at pH 4.0 and 5.0. The most intense chirality is observed at pH 4.0, where CND forms more compact assemblies with alginate. MD simulations suggest a different spatial organization of CND with pH: cationic forms at pH below 3.6 should arrange with their charges parallel pointing out towards the alginate, while non charged CND should display a crossed arrangement, which is probably responsible for strong signal observed in the CD spectra in this condition, with the intensity of the CD signal increasing with the sinus of the angle between the transition dipole moments of the two chromophores. While conclusive proof of the spatial arrangement of CND in CND/alginate complexes was not obtained, the organization of CND suggested by MD simulations explains some of the features of the complexes observed our experimental work.

4. Conclusions

The interaction of CND with alginate is strongly influenced by pH for the range of pHs shown in this work, from 2.5 to 5.0. The complexation of CND with alginate favours CND association through dimerization, resulting in interesting chiral properties. CD spectra from the complexes show features with pH very different from free CND in solution with respect to intensity and sign of the bands of the spectra. UV spectra suggest that CND is present predominantly in the hemiketal and neutral quinoid base forms in the complexes at pHs over 3.6. These forms, not charged, could allow for the formation of larger CND aggregates, which could explain the fibrillar structure and the fractal arrangement of the complexes at pH 4.0 and 5.0. At pH 3.0 the complexes behave as a disordered polymer, and chiral properties are similar to those of free CND. At acidic pHs the positive charge of the predominant flavylium ion must prevent large association of the CND over dimers. MD simulations hint at a crossed arrangement of CND molecules in dimers at pH 4.0, whereas at pH 3.0, CND must form parallel dimers.

CRediT authorship contribution statement

Nattida Chotechuang: Investigation, Methodology. **Paolo Di Gianvincenzo**: Investigation, Methodology, Writing – Original Draft. **Cheng Giuseppe Chen**: Methodology, Formal analysis. **Alessandro Nicola Nardi**: Methodology, Formal analysis. **Daniel Padró**: Investigation. **Chanchai Boonla**: Supervision. **Maria Grazia Ortore**: Investigation. **Marco D' Abramo**: Supervision, Formal analysis. **Sergio E. Moya**: Conceptualization, Supervision, Writing – Original Draft.

Declaration of competing interest

Authors have no competing interests to declare.

Acknowledgements

The authors thank the CERIC-ERIC Consortium for the access to experimental facilities of Elettra Synchrotron and Heinz Amenitsch for SAXS beamline set-up. . S.E.M. thanks the PID2020-114356RB-I00 project from the Ministry of Science and Innovation of the Government of Spain. This work was performed under the Maria de Maeztu Units of Excellence Program from the Spanish State Research Agency—Grant No. MDM-2017-0720. Julia Cope, PhD of CIC biomaGUNE proofread the manuscript before submission.

References

Abraham, M. J., Murtola, T., Schulz, R., Páll, S., Smith, J. C., Hess, B., & Lindahl, E. (2015). GROMACS: High performance molecular simulations through multi-level parallelism from laptops to supercomputers. *SoftwareX*, *1–2*, 19–25. https://doi.org/10.1016/j.softx.2015.06.001

Asen, S., Stewart, R. N., & Norris, K. H. (1972). Co-pigmentation of anthocyanins in plant tissues and its effect on color. *Phytochemistry*, *11*(3), 1139–1144. https://doi.org/10.1016/S0031-9422(00)88467-8

Beaucage, G. (1996). Small-Angle scattering from polymeric mass fractals of arbitrary mass-fractal dimension. *Journal of Applied Crystallography*, *29*(2), 134–146. https://doi.org/10.1107/S0021889895011605

Burian, M., Meisenbichler, C., Naumenko, D., & Amenitsch, H. (2022). *SAXSDOG* : open software for real-time azimuthal integration of 2D scattering images. *Journal of Applied Crystallography*, *55*(3), 677–685. https://doi.org/10.1107/S1600576722003685

Bussi, G., Donadio, D., & Parrinello, M. (2007). Canonical sampling through velocity rescaling. *The Journal of Chemical Physics*, *126*(1), 014101. https://doi.org/10.1063/1.2408420

Cantor, C. R., & Schimmel, P. R. (1980). *Biophysical Chemistry. Part II, Techniques for the study of biological structure and function*. New York: W.H. Freeman and Company Chapter 8.

Chai, J.-D., & Head-Gordon, M. (2008). Long-range corrected hybrid density functionals with damped atom–atom dispersion corrections. *Physical Chemistry Chemical Physics*, *10*(44), 6615. https://doi.org/10.1039/b810189b

Dangles, O., & Fenger, J.-A. (2018). The chemical reactivity of anthocyanins and its consequences in food science and nutrition. *Molecules*, *23*(8), 1970. https://doi.org/10.3390/molecules23081970

Darden, T., York, D., & Pedersen, L. (1993). Particle mesh Ewald: An *N* ·log(*N*) method for Ewald sums in large systems. *The Journal of Chemical Physics*, *98*(12), 10089–10092. https://doi.org/10.1063/1.464397

Del Galdo, S., Marracino, P., D'Abramo, M., & Amadei, A. (2015). In silico characterization of protein partial molecular volumes and hydration shells. *Physical Chemistry Chemical Physics*, *17*(46), 31270–31277. https://doi.org/10.1039/C5CP05891K

Fernandes, A., Brás, N. F., Oliveira, J., Mateus, N., & de Freitas, V. (2016). Impact of a pectic polysaccharide on oenin copigmentation mechanism. *Food Chemistry*, *209*, 17–26. https://doi.org/10.1016/j.foodchem.2016.04.018

Francis, F. J., & Markakis, P. C. (1989). Food colorants: Anthocyanins. *Critical Reviews in Food Science and Nutrition*, *28*(4), 273–314. https://doi.org/10.1080/10408398909527503

Frisch, M. J., Trucks, G. W., Schlegel, H. B., Scuseria, G. E., Robb, M. A. , Cheeseman, J. R., Scalmani, G., Barone, V., Petersson, H., Nakatsuji, H., Li, X., Caricato, M., Merenich, A. V., Bloino, J., Janesko, B. G., Gomperts, R. et al. (2016). *Gaussian 16, Revision B.01*. Gaussian Inc.

Gavara, R., Petrov, V., Quintas, A., & Pina, F. (2013). Circular dichroism of anthocyanidin 3-glucoside self-aggregates. *Phytochemistry*, *88*, 92–98. https://doi.org/10.1016/j.phytochem.2012.12.011

Hoshino, T., Matsumoto, U., & Goto, T. (1981). Self-association of some anthocyanins in neutral aqueous solution. *Phytochemistry*, *20*(8), 1971–1976. https://doi.org/10.1016/0031-9422(81)84047-2

Hoshino, T., Matsumoto, U., Harada, N., & Goto, T. (1981). Chiral exciton coupled stacking of anthocyanins: interpretation of the origin of anomalous CD induced by anthocyanin

association. *Tetrahedron Letters*, *22*(37), 3621–3624. https://doi.org/10.1016/S0040-4039(01)81976-6

Houbiers, C., Lima, J. C., Maçanita, A. L., & Santos, H. (1998). Color Stabilization of Malvidin 3-Glucoside: Self-Aggregation of the Flavylium Cation and Copigmentation with the *Z* -Chalcone Form. *The Journal of Physical Chemistry B*, *102*(18), 3578–3585. https://doi.org/10.1021/jp972320j

Houghton, A., Appelhagen, I., & Martin, C. (2021). Natural blues: Structure meets function in anthocyanins. *Plants*, *10*(4), 726. https://doi.org/10.3390/plants10040726

Jeoh, T., Wong, D. E., Strobel, S. A., Hudnall, K., Pereira, N. R., Williams, K. A., Arbaugh, B. M., Cunniffe, J. C., & Scher, H. B. (2021). How alginate properties influence in situ internal gelation in crosslinked alginate microcapsules (CLAMs) formed by spray drying. *PLOS ONE*, *16*(2), e0247171. https://doi.org/10.1371/journal.pone.0247171

Jo, S., Kim, T., Iyer, V. G., & Im, W. (2008). CHARMM-GUI: A web-based graphical user interface for CHARMM. *Journal of Computational Chemistry*, *29*(11), 1859–1865. https://doi.org/10.1002/jcc.20945

Leydet, Y., Gavara, R., Petrov, V., Diniz, A. M., Jorge Parola, A., Lima, J. C., & Pina, F. (2012). The effect of self-aggregation on the determination of the kinetic and thermodynamic constants of the network of chemical reactions in 3-glucoside anthocyanins. *Phytochemistry*, *83*, 125–135. https://doi.org/10.1016/j.phytochem.2012.06.022

Oidtmann, J., Schantz, M., Mäder, K., Baum, M., Berg, S., Betz, M., Kulozik, U., Leick, S., Rehage, H., Schwarz, K., & Richling, E. (2012). Preparation and comparative release characteristics of three anthocyanin encapsulation systems. *Journal of Agricultural and Food Chemistry*, *60*(3), 844–851. https://doi.org/10.1021/jf2047515

Olivas-Aguirre, F., Rodrigo-García, J., Martínez-Ruiz, N., Cárdenas-Robles, A., Mendoza-Díaz, S., Álvarez-Parrilla, E., González-Aguilar, G., de la Rosa, L., Ramos-Jiménez, A., & Wall-Medrano, A. (2016). Cyanidin-3-O-glucoside: Physical-chemistry, foodomics and health effects. *Molecules*, *21*(9), 1264. https://doi.org/10.3390/molecules21091264

Pina, F. (2014). Chemical applications of anthocyanins and related compounds. A source of bioinspiration. *Journal of Agricultural and Food Chemistry*, *62*(29), 6885–6897. https://doi.org/10.1021/jf404869m

Pina, F., Melo, M. J., Laia, C. A. T., Parola, A. J., & Lima, J. C. (2012). Chemistry and applications of flavylium compounds: a handful of colours. *Chemical Society Reviews*, *41*(2), 869–908. https://doi.org/10.1039/C1CS15126F

Polizzi, S., Spinozzi, F. (2015). Small Angle X-Ray Scattering (SAXS) with Synchrotron Radiation Sources. In: Mobilio, S., Boscherini, F., Meneghini, C. (eds) Synchrotron Radiation. Springer, Berlin, Heidelberg. https://doi.org/10.1007/978-3-642-55315-8_11

Quina, F. H., Moreira, P. F., Vautier-Giongo, C., Rettori, D., Rodrigues, R. F., Freitas, A. A., Silva, P. F., & Maçanita, A. L. (2009). Photochemistry of anthocyanins and their biological role in plant tissues. *Pure and Applied Chemistry*, *81*(9), 1687–1694. https://doi.org/10.1351/PAC-CON-08-09-28

Rupasinghe, H. P. V., Arumuggam, N., Amararathna, M., & de Silva, A. B. K. H. (2018). The potential health benefits of haskap (Lonicera caerulea L.): Role of cyanidin-3- O -glucoside. *Journal of Functional Foods*, *44*, 24–39. https://doi.org/10.1016/j.jff.2018.02.023

Singh, U. C., & Kollman, P. A. (1984). An approach to computing electrostatic charges for molecules. *Journal of Computational Chemistry*, *5*(2), 129–145. https://doi.org/10.1002/jcc.540050204

Spinozzi, F., Ferrero, C., Ortore, M. G., de Maria Antolinos, A., & Mariani, P. (2014). *GENFIT* : software for the analysis of small-angle X-ray and neutron scattering data of macromolecules in solution. *Journal of Applied Crystallography*, *47*(3), 1132–1139. https://doi.org/10.1107/S1600576714005147

Trouillas, P., Sancho-García, J. C., de Freitas, V., Gierschner, J., Otyepka, M., & Dangles, O. (2016). Stabilizing and Modulating Color by Copigmentation: Insights from Theory and Experiment. *Chemical Reviews*, *116*(9), 4937–4982. https://doi.org/10.1021/acs.chemrev.5b00507

Vanommeslaeghe, K., Hatcher, E., Acharya, C., Kundu, S., Zhong, S., Shim, J., Darian, E., Guvench, O., Lopes, P., Vorobyov, I., & Mackerell, A. D. (2010). CHARMM general force field: A force field for drug-like molecules compatible with the CHARMM all-atom additive biological force fields. *Journal of Computational Chemistry*, NA-NA. https://doi.org/10.1002/jcc.21367

Yi, W., Akoh, C. C., Fischer, J., & Krewer, G. (2006). Absorption of Anthocyanins from Blueberry Extracts by Caco-2 Human Intestinal Cell Monolayers. *Journal of Agricultural and Food Chemistry*, *54*(15), 5651–5658. https://doi.org/10.1021/jf0531959

Zou, C., Huang, L., Li, D., Ma, Y., Liu, Y., Wang, Y., Cao, M.-J., Liu, G.-M., & Sun, L. (2021). Assembling cyanidin-3-O-glucoside by using low-viscosity alginate to improve its in vitro bioaccessibility and in vivo bioavailability. *Food Chemistry*, *355*, 129681. https://doi.org/10.1016/j.foodchem.2021.129681

Credit author stament

Nattida Chotechuang: Investigation, Methodology. **Paolo Di Gianvincenzo**: Investigation, Methodology, Writing – Original Draft. **Cheng Giuseppe Chen**: Methodology, Formal analysis. **Alessandro Nicola Nardi**: Methodology, Formal analysis. **Daniel Padró**: Investigation. **Chanchai Boonla**: Supervision. **Maria Grazia Ortore**: Investigation. **Marco D' Abramo**: Supervision, Formal analysis. **Sergio E. Moya**: Conceptualization, Supervision, Writing – Original Draft.

Declaration of interests

☒ The authors declare that they have no known competing financial interests or personal relationships that could have appeared to influence the work reported in this paper.

☐ The authors declare the following financial interests/personal relationships which may be considered as potential competing interests:

Journal Pre-proof

Graphical abstract

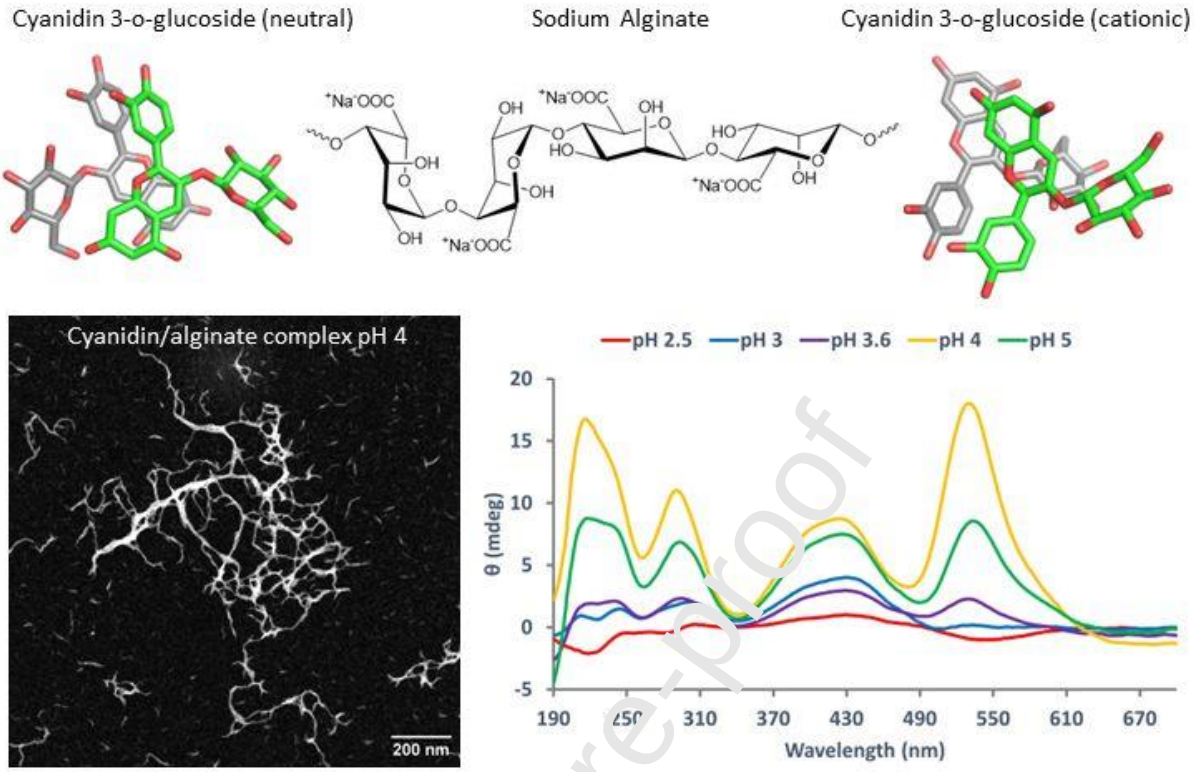

Journal Pre-proof